Clim. Past Discuss., 9, 4745–4770, 2013
www.clim-past-discuss.net/9/4745/2013/
doi:10.5194/cpd-9-4745-2013

Climate of the Past Discussions
Open Access

What controls deuterium excess in global precipitation?

S. Pfahl and H. Sodemann

Institute for Atmospheric and Climate Science, ETH Zurich, 8092 Zurich, Switzerland

Received: 25 July 2013 – Accepted: 7 August 2013 – Published: 14 August 2013

Correspondence to: S. Pfahl (stephan.pfahl@env.ethz.ch) and
H. Sodemann (harald.sodemann@env.ethz.ch)

Published by Copernicus Publications on behalf of the European Geosciences Union.

Abstract

The deuterium excess (d) of precipitation is widely used in the reconstruction of past climatic changes from ice cores. However, its most common interpretation as moisture source temperature cannot directly be inferred from present-day water isotope observations. Here, we use a new empirical relation between d and near-surface relative humidity together with reanalysis data to globally predict d of surface evaporation from the ocean. The very good quantitative agreement of the predicted hemispherically averaged seasonal cycle with observed d in precipitation indicates that moisture source relative humidity, and not sea surface temperature, is the main driver of d variability on seasonal time scales. There is no convincing evidence that RH might be less important for long-term palaeoclimatic d changes compared to moisture source temperature variations. Ice core d data may thus have to be reinterpreted, focusing on climatic influences on relative humidity during evaporation, in particular related to atmospheric circulation changes.

1 Introduction

Stable water isotopes in atmospheric waters are useful tracers of the global hydrological cycle (Dansgaard, 1964; Gat, 1996), and their conservation in proxy archives like ice cores and cave deposits is essential for the reconstruction of past climates (e.g. Jouzel et al., 1982; Dansgaard et al., 1993; Meckler et al., 2012). The deuterium excess, defined as $d = \delta\mathrm{D} - 8\delta^{18}\mathrm{O}$ (where $\delta\mathrm{D}$ and $\delta^{18}\mathrm{O}$ denote the deuterium and oxygen-18 abundance relative to VSMOW), is a second-order isotope parameter that is specifically sensitive to the conditions during the evaporation of water from the (ocean) surface, i.e., the moisture source conditions (Merlivat and Jouzel, 1979; Johnsen et al., 1989; Pfahl and Wernli, 2008). Accordingly, d variations in ice cores and other palaeoclimatic proxy archives are thought to reflect past changes in these source conditions (Jouzel et al., 1982; Vimeux et al., 1999; Stenni et al., 2001; Masson-Delmotte et al.,

CPD
9, 4745–4770, 2013

2005; Jouzel et al., 2007; Steffensen et al., 2008). Deuterium excess has become a key parameter for studying climate variations, in particular abrupt events recorded in the proxy data (Jouzel et al., 2007; Steffensen et al., 2008). In stable isotope data from Greenland ice cores, rapid (1–3 yr) changes in d have been interpreted as fast reorganisations in the atmospheric circulation associated with changes in the moisture source conditions (Steffensen et al., 2008) and/or locations (Masson-Delmotte et al., 2005). Despite the general sparsity of isotope measurements in evaporating waters a theoretical framework for the interpretation of d could be derived, which is briefly revisited in the following.

Physically, the deuterium excess reflects the slower movement of the $H_2^{18}O$ molecule during diffusion, leading to a relative enrichment of the HDO molecules in the less strongly bound phase (e.g., in the gas phase during the evaporation of water). This slower movement can only lead to measurable differences if there is not sufficient time for the two phases to reach isotopic equilibrium. During evaporation, such non-equilibrium conditions are caused by a strong gradient in relative humidity above the water surface, and by winds that advect the evaporate away from the surface before (near-)equilibrium conditions between the two phases can be reached. Following Craig and Gordon (1965) and Merlivat and Jouzel (1979), the isotopic composition δ_E^i of water evaporating from the ocean for the isotopic species i ($i = {}^{18}O$, D) can be expressed as

$$1 + \delta_E^i = (1 - k_i)\frac{\alpha_i^{-1}\mathrm{RH}(1 + \delta_v^i)}{1 - \mathrm{RH}}, \quad (1)$$

where RH is the relative humidity with respect to saturation at the sea surface, δ_v^i is the isotopic composition of the surrounding vapour for species i, α_i is the temperature-dependent equilibrium fractionation factor, and k_i is the non-equilibrium (diffusive) fractionation factor. The exact formulation of this non-equilibrium fractionation factor as a function of wind speed and potentially temperature is still under discussion (Pfahl and Wernli, 2009; Luz et al., 2009). For analysing variations of d on global scales,

CPD
9, 4745–4770, 2013

Merlivat and Jouzel (1979) introduced a global closure assumption in which the isotopic composition of the surrounding vapour δ_v^i was assumed to be equal to the isotopic composition of global precipitation, which in turn equals the isotopic composition of global evaporation. This allowed to derive a simplified expression for the isotope ratio in water vapour from evaporation:

$$\delta_v^i = \alpha_i^{-1} \frac{1 - k_i}{1 - k_i \mathrm{RH}} - 1. \quad (2)$$

However, as pointed out by Jouzel and Koster (1996), this global closure assumption is typically invalid on local scales. Jouzel and Koster (1996) recommend to use climate model data for δ_v^i in Eq. (1), which are associated with uncertainties regarding the representation of d though (Yoshimura et al., 2008; Risi et al., 2010; Jouzel et al., 2007). Equation (2) can be combined for both isotopes to obtain an expression for d in boundary layer water vapour and thus (implying global closure) in water evaporating from the ocean. Using a simple Rayleigh condensation model, Merlivat and Jouzel (1979) derived a strong dependency of d on RH in the so-called first condensate, the initial precipitation, while the influence of evaporation temperature remained indistinguishable. The later study by Johnsen et al. (1989) directly used the isotopic composition derived from the global closure (Eq. 2) to estimate d locally at an assumed fixed moisture source for Greenland from monthly mean RH and sea surface temperature (SST) values. Thereby simple linear relations can be derived between changes in RH and SST and d in the water evaporating from the ocean:

$$\frac{\Delta d}{\Delta \mathrm{SST}} = +0.35 \frac{‰\, d}{\mathrm{K\,SST}}$$
$$\frac{\Delta d}{\Delta \mathrm{RH}} = -0.43 \frac{‰\, d}{\%\,\mathrm{RH}}. \quad (3)$$

RH is a direct factor of influence in Eq. (2), while SST affects the temperature-dependent equilibrium fractionation factors α_i. According to Eq. (3) d becomes higher

CPD
9, 4745–4770, 2013

with increasing SST and lower with increasing RH, with constants of proportionality of comparable magnitude. Nevertheless, on synoptic time scales, the dependence of d on SST is substantially weaker than on RH, because the variability of RH in % typically is much larger than the variability of SST in K. It is common to most studies until now that RH has been considered at relatively long averaging times, compared to the time scale at which evaporation actually takes place, thereby substantially underestimating the variability of RH. From their study with an idealised model, and using monthly mean data for the initialisation, Johnsen et al. (1989) concluded that SST and RH changes could both play a role for d variations observed in a Greenland ice core. Noting that GCM simulations show only small glacial-to-interglacial changes in mean oceanic RH, it has been proposed that d in Antarctic ice core records can be interpreted as moisture source SST signal only (Vimeux et al., 1999; Stenni et al., 2001; Uemura et al., 2012), revoking the earlier interpretation as a proxy of moisture source RH (Jouzel et al., 1982). This interpretation as source SST has later been extended also to Greenland ice cores (Masson-Delmotte et al., 2005). In recent climate model studies, Lewis et al. (2013) and Risi et al. (2012) investigated the relationship between d and moisture source conditions on different time scales. Lewis et al. (2013) focused on the role of SST, but noted that source RH changes might introduce errors in the d-SST relation. Risi et al. (2012) discussed several factors controlling d variations, including moisture source RH and SST, and emphasised the potential impacts of model uncertainties for the interpretation of these variations.

Recent measurements of d in boundary layer water vapour consistently show that at synoptic time scales (from hours to days), RH above the ocean surface is highly anti-correlated with d in atmospheric water vapour (Gat et al., 2003; Uemura et al., 2008; Angert et al., 2008; Pfahl and Wernli, 2008; Kurita, 2011). Interestingly, when plotted together against source RH, the d measurements from these studies (Gat et al., 2003; Uemura et al., 2008; Angert et al., 2008; Pfahl and Wernli, 2008) fall on one line (Fig. 1a) although they are from such different geographical regions as the Southern Ocean and the Mediterranean, span a wide range of evaporation conditions, and have

CPD
9, 4745–4770, 2013

been obtained with different approaches (see Sect. 2). This, consistently with theoretical considerations (Merlivat and Jouzel, 1979; Craig and Gordon, 1965), points to a universal relationship between d of water evaporating from the ocean and the corresponding near-surface RH. In this study, we apply this relationship in a linear statistical model to globally predict d of the evaporating water. In this way, we avoid the global closure assumption inherent in simple theoretical evaluations (see again Eq. 2) and the uncertainties related to the representation of d in climate models. By using six-hourly RH from ERA-Interim reanalyses (Dee et al., 2011) as predictor, the model explicitly considers the synoptic-scale processes that drive short-term RH variations. On these time scales, RH and wind speed are the main factors determining oceanic evaporation. The empirical relation applied in our model relates d linearly to a standard meteorological quantity, a linkage that does not directly emerge from theoretical derivations. By comparing the predicted d in evaporation with d measurements in precipitation, we evaluate the relevance of the d-RH relationship for global precipitation data.

2 Data and methods

The statistical model that relates the deuterium excess of water evaporating from the ocean to the near-surface RH is based on several sets of measurements of d in atmospheric water vapour from the literature (Gat et al., 2003; Uemura et al., 2008; Angert et al., 2008). Gat et al. (2003) performed daily measurements of the isotopic composition of near-surface water vapour on board a ship during a one month cruise over the Mediterranean Sea in 1995. The measurements were done at mast and deck height, and the deck data have been used here. Furthermore, measurements have been discarded if precipitation occurred in the vicinity of the ship. Uemura et al. (2008) also measured isotopes in vapour on board a ship, with a measurement frequency of 2–3 times per day. Their cruise took place over the Southern Ocean, from South Africa towards Antarctica and to Australia, in January 2006. Angert et al. (2008) performed isotope measurements in water vapour over 9 yr (sampling about two times a week) at

CPD
9, 4745–4770, 2013

a near-coastal site in Rehovot, Israel. Here only those data have been used for which most of the sampled vapour could be traced backed to oceanic evaporation sources with the trajectory method of Pfahl and Wernli (2008). RH is defined with respect to saturation at the sea surface here (as in Eq. 1), i.e., RH = q/q_{sat}(SST), where q denotes the specific humidity above the ocean surface, and q_{sat}(SST) is the saturation humidity at the surface. For ship data from the Mediterranean (Gat et al., 2003) and the Southern Ocean (Uemura et al., 2008), q and SST have been used as observed in-situ. Thereby, vapour over the ocean has been assumed to be directly associated with local evaporation. For the station data from Israel (Angert et al., 2008), q and SST in the moisture source regions were reconstructed by means of a trajectory method (see again Pfahl and Wernli, 2008). Figure 1a shows d from all three data sets, plotted against RH. A linear regression has been used to model the relationship between d in ocean evaporation and the near-surface RH, as indicated by the solid red line, which corresponds to the equation $d = 48.2‰ - 0.54‰\%^{-1}$ RH. The dashed lines show the 95 % confidence intervals of the linear regression. This regression model has then been applied to predict d of water evaporating from the ocean, using RH from meteorological reanalysis data as input.

To this end, six-hourly, global fields of specific humidity at 2 m above the surface (calculated from 2 m temperature and dew point temperature) and SST for the period 1979–2010 have been obtained from ECMWF ERA-Interim reanalyses (Dee et al., 2011). The data have been interpolated to a $1^\circ \times 1^\circ$ spatial grid. RH above the ocean surface has then been calculated as described above. In addition, sea ice cover, surface latent heat flux and land surface temperature have also been taken from the reanalysis data. The latent heat flux is a forecast field, and forecast steps from 6 to 12 and 12 to 18 h are used, neglecting the first six hours because of possible model spin-up effects. The linear regression model described above has been applied to calculate d of water evaporating from the ocean for each six-hourly time step and each grid point, taking the reanalysis RH as input. The uncertainty of the linear regression is used as an uncertainty estimate for predicted d. Note that this estimate does not account for the

CPD
9, 4745–4770, 2013

uncertainties of the individual d and RH measurements and should thus be considered as lower bound of the model uncertainty. Taking errors of individual data points into account is hardly possible, since these depend on various factors such as the related moisture source footprint. Climatological means of d have been obtained at every grid point and for each month and season by averaging the corresponding six-hourly values, weighted with the six-hourly surface latent heat flux. Finally, hemispheric means have been calculated by averaging d over all grid boxes in the respective hemisphere, weighted with the grid box surface area and mean latent heat flux. The weighting with evaporation/latent heat flux is necessary to compare with the precipitation-weighted GNIP data (see below) and to close the d budget of the atmospheric water cycle.

In order to evaluate our model, measurements of d in monthly precipitation from the Global Network of Isotopes in Precipitation (GNIP) (IAEA, 2006; Araguás-Araguás et al., 2000) have been employed. All stations have been considered for which at least 36 months of data of δD, δ^{18}O and precipitation amount were available during the period 1960–2009. Precipitation-weighted climatological means of d for every calendar month and season have been calculated at each station with at least three observations from the respective month, or nine from the respective season. To obtain hemispheric means of d in precipitation, station data have first been averaged over $10^\circ \times 10^\circ$ grid boxes, then the grid box mean values have been averaged zonally and meridionally, weighted by the grid box sizes and mean precipitation amounts. The hemispheric means obtained in this way are in good agreement with the results of Araguás-Araguás et al. (2000), who used a similar dataset. Assuming only little moisture exchange between the hemispheres, the hemispheric means of d in precipitation and ocean evaporation, according to the global closure assumption (see Sect. 1), should be equal when averaged over sufficiently long time periods.

CPD
9, 4745–4770, 2013

3 Results and discussion

3.1 Deuterium excess and relative humidity

Figure 1b shows the predicted mean seasonal cycle of d in ocean evaporation from our statistical model, averaged over the Northern Hemisphere (NH) and Southern Hemisphere (SH). Both curves have a maximum in winter, and the amplitude of the seasonal cycle is larger in the NH than in the SH. The model results are in very good quantitative agreement with the hemispherically averaged GNIP data. The close correspondence with respect to phase, amplitude, and absolute values is striking given that our model is fully independent from the precipitation data. In the NH, the seasonal cycle of d in precipitation has a slightly smaller amplitude compared to the statistical model. This is likely caused by the fact that the residence time of water over the continents is often larger than one month (Numaguti, 1999), which induces a smoothing of the seasonal cycle in continental precipitation. In the SH, the model has a negative bias of 1–2 ‰ compared to the precipitation data. This may be due to the sparse spatial coverage of GNIP stations; there are no data, e.g., over large parts of the Southern Ocean where evaporation d is relatively high (see below).

The seasonally averaged spatial patterns of d in moisture evaporating from the ocean that are obtained from our model also reflect the strong seasonality in the NH, and a weaker, opposite signal in the SH (Fig. 2, shading). The spatial patterns are strongly related to evaporation-weighted RH over the ocean (Fig. 3a, b). During NH winter, high values of d are predicted downstream (i.e., to the east) of North America and East Asia, associated with intense oceanic evaporation (cf. Fig. 3e, f) into dry continental air masses advected over the adjacent oceans with the mean westerly circulation (Fig. 2a, red colours). The large humidity gradients over the sea surface lead to strong non-equilibrium fractionation resulting in high d values. A further maximum of d is predicted in the region of the Barents Sea. In the SH winter, maxima of d are found near the sea ice edge, and at the coast of Australia (Fig. 2b). The weaker seasonality of d in the SH is likely due to the absence of large midlatitude continental areas. Hence,

CPD
9, 4745–4770, 2013

while induced by oceanic RH in both hemispheres, *d* in precipitation appears to be influenced by the differing land-sea distribution.

Several large-scale spatial features of predicted *d* in ocean evaporation are also reflected in the seasonally averaged precipitation data from GNIP stations (circles in Fig. 2). The zonal gradient of evaporation *d* across the main ocean basins in the NH during winter is mirrored by higher precipitation *d* in the eastern than in the western parts of the North American and the Eurasian continents (Fig. 2a). Very high precipitation *d* is observed at eastern Mediterranean stations in NH winter, reflecting the high *d* in water evaporating from the surrounding seas (Gat et al., 2003). In the SH, Pacific Island stations show lower precipitation *d* than predicted for evaporation, partly causing the offset between measurements and model results seen in Fig. 1. To some extent these differences may be due to inter-annual variability, since several stations only cover a limited number of years.

Despite the similarities between predicted evaporation and measured precipitation *d*, it is important to keep in mind that at a single location precipitation *d* is also affected by variations in the moisture source regions, and by secondary effects such as differences in the isotopic composition of the ocean source as well as isotopic fractionation during the progressive cooling of an air mass, during ice cloud formation and during the evaporation of rain drops and soil water (Jouzel and Merlivat, 1984; Jouzel et al., 2007). Such secondary effects are particularly important at high latitudes, where most of the precipitation falls as snow. Due to mass conservation, the secondary effects cancel out if long-term hemispheric averages are considered, as demonstrated by the good correspondence between predicted *d* in ocean evaporation and GNIP precipitation data (Fig. 1b). The primary influence on local-scale variability of precipitation *d* is the seasonal and spatial variation of moisture sources, which can be large (Sodemann et al., 2008b; Sodemann and Zubler, 2010). Sophisticated methods for diagnosing moisture source regions hence have to be applied to fully explain *d* in precipitation at individual stations in terms of the moisture source RH (Sodemann et al., 2008a; Pfahl and Wernli, 2008, 2009), in particular for continental stations, as is the case for a substantial part of

CPD
9, 4745–4770, 2013

the GNIP network. In turn, the relationship between d and RH opens the possibility to constrain such model-based moisture source diagnostics. In addition, changes in moisture transport induced by climate change, which can lead to variations in regional-scale moisture budgets, may be quantifiable through their d fingerprint.

In summary, this comparison shows that there is a close correspondence between hemispherically averaged seasonal cycles of predicted d in evaporation and measurements of d in precipitation. Near-surface relative humidity is used as sole predictor of evaporation d, and thus the seasonal cycles of d and RH are linearly related (Fig. 4). In turn, there is a close in-phase relationship between the seasonal cycles of RH and the average temperature above land areas (Fig. 4), which reflects the surface radiation balance. With regard to the spatial patterns of d in ocean evaporation and precipitation, there is some correspondence of large-scale features, but there are also differences on local scales due to variations in moisture source regions and processes not taken into account in our simple model, like the formation of ice clouds.

3.2 Potential influence of SST

The conspicuous agreement of our model results with GNIP measurement data shows that the linear relationship between d and moisture source RH, which has been derived from observations on (sub-)daily time scales and captures a fundamental isotopic process during ocean evaporation, also dominates seasonal variations of d in precipitation on a hemispheric scale. In contrast, there is much less resemblance between d and SST, both spatially and temporally: the spatial distribution of SST (Fig. 3c, d) has a much stronger meridional gradient and less zonal variability compared to observed d in precipitation. A phase shift between the hemispherically averaged seasonal cycles of the two variables exists (Fig. 4, black and blue lines). The positive correlation of d and SST usually assumed in palaeoclimatological reconstructions (Johnsen et al., 1989; Vimeux et al., 1999; Masson-Delmotte et al., 2005, see also Eq. 3) is at odds with the timing of the respective seasonal cycles. Also on a daily time scale a much

CPD
9, 4745–4770, 2013

weaker correlation and much less resemblance to a linear relation is found between d and SST (Fig. 5) compared to d and RH (cf. Fig. 1a).

Nevertheless, all these findings are based on the analysis of present-day climate, and it is not guaranteed that the relation between d and RH also dominates long-term palaeoclimatic d variations. Many previous studies have interpreted such d variations in terms of moisture source temperature (see Sect. 1). They have presented different arguments for this interpretation, which we would like to discuss in the following.

- Vimeux et al. (1999) argued that changes of RH over the Southern Ocean between glacial and present-day climate simulated by GCMs are typically small. In addition, global-scale changes of RH are constrained to small values by the surface energy budget (Schneider et al., 2010). However, even if mean RH stays constant, the d-RH relationship may yet be associated with d variations in proxy archives. For example, if the moisture sources of an ice core shift from regions with high to regions with low RH (e.g., from the western to the eastern North Atlantic), this may cause huge changes in the resulting precipitation d. Similarly, shifts in precipitation seasonality (Krinner et al., 1997; Werner et al., 2000) may lead to large variations in annual mean d due to the strong seasonal cycle of d at the evaporation source. In addition, also if global mean changes in RH are small, local variations can occur, e.g., due to changes in sea ice cover, land-sea temperature contrast or storm tracks.

- Uemura et al. (2008) found a positive correlation between d and SST in measurements along a ship cruise from South Africa to the sea ice edge and back towards Australia. However, the spatial patterns of RH, SST and d shown in Figs. 3a, c and 2a suggest that this may be explained by cross-correlation with RH (positive gradient of RH and negative gradient of SST along parts of the ship track) and thus does not represent an independent confirmation of the effect of SST on d. Other studies based on measurement data (Gat et al., 2003; Pfahl and Wernli, 2008) even found a negative relationship between d and SST (cf. Fig. 5).

CPD
9, 4745–4770, 2013

– The d–RH relationship would translate into a positive correlation between d and SST (as widely assumed in the interpretation of ice cores) if variations of SST and RH were always anti-correlated. However, there is no such systematic anti-correlation of SST and RH in observations. On short, daily time scales, RH and near-surface air temperature time series are correlated in the extratropics and anti-correlated in the tropics (Pfahl and Niedermann, 2011). If SST is considered instead of near-surface air temperature, these (anti-)correlations are generally much weaker, since the magnitude of daily SST variations is smaller than for air temperature (not shown). Also on longer, inter-annual time scales there is no systematic covariance between near-surface RH and temperature time series (Fig. 18b of Dai, 2006). Figure 6 shows scatter plots of d from our empirical model plotted against SST at the respective grid points. Since the model is linear, the same patterns are obtained if RH is used instead of d. No systematic relationship between d (RH) and SST can be found in these plots, indicating that the first-order relationship between d and RH, which has been used to construct the model, does not translate into a simple correlation of d and SST. All together, this demonstrates the complexity of the relation between RH and SST. We are not aware of (and do not forsee) a physical argument which could evoke a direct anti-correlation between long-term changes of the two variables.

– Johnsen et al. (1989) used the phase shift between the seasonal cycles of d and δ^{18}O in Greenland ice as an indicator of the effects of SST on d. However, the seasonal d cycles from shallow ice cores form the NEEM site, Greenland (Steen-Larsen et al., 2011) and Law Dome, Antarctica (Delmotte et al., 2000) do not correspond with the seasonal cycle of SST (Fig. 4, dashed and blue lines). On the contrary, there is a good agreement between the NEEM data and our hemispheric-mean model predictions (black solid lines). At Law Dome, the signal is more variable, pointing to a larger influence of local factors.

CPD
9, 4745–4770, 2013

– Recent climate model studies suggest that long-term *d* variations throughout the Holocene may be related to SST changes to some degree (Lewis et al., 2013). However, different models seem not to show consistent results (cf. Risi et al., 2012), and such conclusion may be affected by model errors. Isotope-enabled GCMs still have difficulties to properly represent the spatial and temporal variability of *d* (Yoshimura et al., 2008; Risi et al., 2010; Jouzel et al., 2007). Recent improvements in the ECHAM5-wiso model are partly due to tuning of the supersaturation function used in the parameterisation of ice clouds (Werner et al., 2011). The large sensitivity of modelled *d* to this tuning (see again Risi et al., 2012) may lead to additional problems: a supersaturation function tuned for present-day climate does not necessarily represent, e.g., last glacial maximum conditions correctly. Future studies on this issue may make use of a prognostic representation of supersaturation in ice clouds that does not require such tuning (Pfahl et al., 2012). In general, models should be thoroughly validated to properly represent the RH–*d* relationship that controls present-day seasonal *d* variations. Being available with high temporal and spatial resolution, *d* from our model can be used as a benchmark for such simulations.

All together, we do not perceive how SST could become a decisive factor for *d* on longer time scales. It does thus not appear justified to neglect the influence of RH on palaeoclimatic *d* variations and to interpret *d* as a proxy for moisture source SST.

4 Conclusions

In this paper, the relationship between *d* and moisture source RH under present-day climate conditions has been studied with the help of a simple, linear empirical model. We have shown that the *d*–RH relation observed on daily time scales also explains the seasonal cycle of hemispherically averaged *d* in precipitation and several large-scale features of its spatial distribution. With respect to the interpretation of *d* proxy records, this relationship between *d* and RH can serve as a first order interpretation guide. It

CPD
9, 4745–4770, 2013

suggests that d variations from proxy records could be used to reconstruct RH during evaporation, which is strongly affected by variations in atmospheric circulation and the corresponding changes of moisture source locations. This first order interpretation is in analogy to the classical temperature effect: spatial and temporal correlations between isotope ratios (δD and δ^{18}O) and temperature have been observed under present-day climate conditions (Dansgaard, 1964) and were subsequently used to link isotope signals from proxy archives to past temperature variations (e.g. Dansgaard et al., 1993). Nevertheless, for a detailed and quantitative analysis of isotope proxy data from individual locations, additional processes have to be taken into account. Regarding the classical temperature effect, e.g., variations in precipitation seasonality and moisture source temperature can influence the relationship between isotope ratios and temperature at the proxy location (Krinner et al., 1997; Werner et al., 2000; Masson-Delmotte et al., 2005). Precipitation seasonality can also impact d because of the large seasonal variability of RH over the ocean. In addition, the d–RH relation may be affected by non-equilibrium fractionation processes during soil evaporation, the re-evaporation of rain drops and, most importantly for ice core locations, the formation of ice clouds (see again Jouzel and Merlivat, 1984; Jouzel et al., 2007). Assessing the relationship between d and moisture source RH is complicated due to its non-local character. In order to fully explore the linkage between d proxy records and moisture source conditions, sophisticated methods thus have to be applied, e.g., using tracer simulations with GCMs (Lewis et al., 2013) or Lagrangian techniques (Sodemann et al., 2008a).

Reinterpreting ice core d as moisture source RH could resolve several complications that have arisen from its previous interpretation as moisture source SST. For example, rapid changes of d in the NGRIP ice core of 2–3 ‰ within 1–3 yr have been interpreted as changes of the moisture source temperature of 2–4 K (Steffensen et al., 2008). Following their interpretation, during the transition from the Younger Dryas (YD) to the Holocene d would decrease, which would imply cooler moisture source temperatures for Greenland in a warmer climate, at least for the beginning of the Holocene (Masson-Delmotte et al., 2005; Steffensen et al., 2008). This counter-intuitive finding

CPD
9, 4745–4770, 2013

was explained by the temporary exposure of cooler ocean areas after the retreat of the sea ice, and fast reorganisations of the atmospheric circulation. Interpreting *d* as driven by RH eliminates the need to involve climate components with inter-annual memory, such as SST and sea ice cover. An alternative explanation of the *d* decrease from the YD to the Holocene would involve reduced land–sea temperature contrasts, relatively more summer precipitation, eastward shifts of the moisture sources in the North Atlantic basin due to a weakened storm track, or a combination of these factors. A combined interpretation of all available data, including GCM studies of past climate states, and the acquisition of new high-resolution isotopic measurements will be crucial to disentangle the interaction between these processes.

Acknowledgements. MeteoSwiss and ECMWF are acknowledged for giving access to ERA-Interim reanalyses, and the IAEA for providing the GNIP data. We are grateful to Nele Meckler and Heini Wernli (ETH Zurich) as well as Valérie Masson-Delmotte (LSCE, IPSL) for helpful comments on an earlier version of the manuscript.

References

Angert, A., Lee, J.-E., and Yakir, D.: Seasonal variations in the isotopic composition of near surface water vapor in the Eastern-Mediterranean, Tellus B, 60, 674–684, doi:10.1111/j.1600-0889.2008.00357.x, 2008. 4749, 4750, 4751

Araguás-Araguás, L., Froehlich, K., and Rozanski, K.: Deuterium and oxygen-18 isotope composition of precipitation and atmospheric moisture, Hydrol. Process., 14, 1341–1355, 2000. 4752

Craig, H. and Gordon, L. I.: Deuterium and oxygen 18 variations in the ocean and the marine atmosphere, in: Stable Isotopes in Oceanographic Studies and Paleotemperatures, edited by: Tongiorgi, E., Lab. Geol. Nucl., Pisa, Italy, 9–130, 1965. 4747, 4750

Dai, A.: Recent climatology, variability, and trends in global surface humidity, J. Climate, 19, 3589–3606, 2006. 4757

Dansgaard, W.: Stable isotopes in precipitation, Tellus B, 16, 436–468, 1964. 4746, 4759

Dansgaard, W., Johnsen, S. J., Clausen, H. B., Dahl-Jensen, D., Gundestrup, N. S., Hammer, C. U., Hvidberg, C. S., Steffensen, J. P., Sveinbjörnsdottir, A. E., Jouzel, J., and Bond, G.:

CPD
9, 4745–4770, 2013

Evidence for general instability of past climate from a 250-kyr ice-core record, Nature, 364, 218–220, 1993. 4746, 4759

Dee, D. P., Uppala, S. M., Simmons, A. J., Berrisford, P., Poli, P., Kobayashi, S., Andrae, U., Balmaseda, M. A., Balsamo, G., Bauer, P., Bechtold, P., Beljaars, A. C. M., van de Berg, L., Bidlot, J., Bormann, N., Delsol, C., Dragani, R., Fuentes, M., Geer, A. J., Haimberger, L., Healy, S. B., Hersbach, H., Holm, E. V., Isaksen, L., Kallberg, P., Koehler, M., Matricardi, M., McNally, A. P., Monge-Sanz, B. M., Morcrette, J.-J., Park, B.-K., Peubey, C., de Rosnay, P., Tavolato, C., Thepaut, J.-N., and Vitart, F.: The ERA-Interim reanalysis: configuration and performance of the data assimilation system, Q. J. Roy. Meteorol. Soc., 137, 553–597, doi:10.1002/qj.828, 2011. 4750, 4751

Delmotte, M., Masson, V., Jouzel, J., and Morgan, V. I.: A seasonal deuterium excess signal at Law Dome, coastal eastern Antarctica: a southern ocean signature, J. Geophys. Res., 105, 7187–7197, 2000. 4757, 4768

Gat, J. R.: Oxygen and hydrogen isotopes in the hydrological cycle, Annu. Rev. Earth Pl. Sc., 24, 225–262, 1996. 4746

Gat, J. R., Klein, B., Kushnir, Y., Roether, W., Wernli, H., Yam, R., and Shemesh, A.: Isotope composition of air moisture over the Mediterranean Sea: an index of the air-sea interaction pattern, Tellus B, 55, 953–965, 2003. 4749, 4750, 4751, 4754, 4756, 4765, 4769

IAEA: Global Network of Isotopes in Precipitation, The GNIP Database, available at: http://www.iaea.org/water (last access: 23 May 2012), 2006. 4752

Johnsen, S. J., Dansgaard, W., and White, J. W. C.: The origin of Arctic precipitation under present and glacial conditions, Tellus B, 41, 452–468, 1989. 4746, 4748, 4749, 4755, 4757

Jouzel, J. and Koster, R. D.: A reconsideration of the initial conditions used for stable water isotope models, J. Geophys. Res., 101, 22933–22938, 1996. 4748

Jouzel, J. and Merlivat, L.: Deuterium and oxygen 18 in precipitation: modeling of the isotope effects during snow formation, J. Geophys. Res., 89, 11749–11757, 1984. 4754, 4759

Jouzel, J., Merlivat, L., and Lorius, C.: Deuterium excess in an East Antarctic ice core suggests higher relative humidity at the oceanic surface during the last glacial maximum, Nature, 299, 688–691, 1982. 4746, 4749

Jouzel, J., Stievenard, M., Johnsen, S. J., Landais, A., Masson-Delmotte, V., Sveinbjörnsdottir, A., Vimeux, F., von Grafenstein, U., and White, J. W. C.: The GRIP deuterium-excess record, Quaternary Sci. Rev., 26, 1–17, 2007. 4747, 4748, 4754, 4758, 4759

CPD
9, 4745–4770, 2013

Krinner, G., Genthon, C., and Jouzel, J.: GCM analysis of local inflluences on ice core δ signals, J. Climate, 24, 2825–2828, doi:10.1029/97GL52891, 1997. 4756, 4759
Kurita, N.: Origin of Arctic vapor during the ice-growth season, Geophys. Res. Lett., 38, L02709, doi:10.1029/2010GL046064, 2011. 4749
Lewis, S. C., LeGrande, A. N., Kelley, M., and Schmidt, G. A.: Modeling insights into deuterium excess as an indicator of water vapor source conditions, J. Geophys. Res., 118, 243–262, doi:10.1029/2012JD017804, 2013. 4749, 4758, 4759
Luz, B., Barkan, E., Yam, R., and Shemesh, A.: Fractionation of oxygen and hydrogen isotopes in evaporating water, Geochim. Cosmochim. Ac., 73, 6697–6703, doi:10.1016/j.gca.2009.08.008, 2009. 4747
Masson-Delmotte, V., Jouzel, J., Landais, A., Stievenard, M., Johnsen, S. J., White, J. W. C., Werner, M., Sveinbjörnsdottir, A., and Fuhrer, K.: GRIP deuterium excess reveals rapid and orbital-scale changes in Greenland moisture origin, Science, 309, 118–121, 2005. 4746, 4747, 4749, 4755, 4759
Meckler, A. N., Clarkson, M. O., Cobb, K. M., Sodemann, H., and Adkins, J. F.: Interglacial hydroclimate in the tropical west Pacific through the late Pleistocene, Science, 336, 1301–1304, doi:10.1126/science.1218340, 2012. 4746
Merlivat, L. and Jouzel, J.: Global climatic interpretation of the deuterium-oxygen 18 relationship for precipitation, J. Geophys. Res., 84, 5029–5033, 1979. 4746, 4747, 4748, 4750
Numaguti, A.: Origin and recycling processes of precipitating water over the Eurasian continent: experiments using an atmospheric general circulation model, J. Geophys. Res., 104, 1957–1972, 1999. 4753
Pfahl, S. and Niedermann, N.: Daily co-variations in near-surface relative humidity and temperature over the ocean, J. Geophys. Res., 116, D19104, doi:10.1029/2011JD015792, 2011. 4757
Pfahl, S. and Wernli, H.: Air parcel trajectory analysis of stable isotopes in water vapor in the eastern Mediterranean, J. Geophys. Res., 113, D20104, doi:10.1029/2008JD009839, 2008. 4746, 4749, 4751, 4754, 4756, 4765, 4769
Pfahl, S. and Wernli, H.: Lagrangian simulations of stable isotopes in water vapor – an evaluation of non-equilibrium fractionation in the Craig-Gordon model, J. Geophys. Res., 114, D20108, doi:10.1029/2009JD012054, 2009. 4747, 4754

CPD
9, 4745–4770, 2013

Pfahl, S., Wernli, H., and Yoshimura, K.: The isotopic composition of precipitation from a winter storm – a case study with the limited-area model $COSMO_{iso}$, Atmos. Chem. Phys., 12, 1629–1648, doi:10.5194/acp-12-1629-2012, 2012. 4758

Risi, C., Bony, S., Vimeux, F., and Jouzel, J.: Water-stable isotopes in the LMDZ4 general circultaion model: model evaluation for present-day and past climates and applications to climatic interpretations of tropical isotopic records, J. Geophys. Res., 115, D12118, doi:10.1029/2009JD013255, 2010. 4748, 4758

Risi, C., Landais, A., Winkler, R., and Vimeux, F.: What controls the spatio-temporal distribution of D-excess and ^{17}O-excess in precipitation? A general circulation model study, Clim. Past Discuss., 8, 5493–5543, doi:10.5194/cpd-8-5493-2012, 2012. 4749, 4758

Schneider, T., O'Gorman, P. A., and Levine, X. J.: Water vapor and the dynamics of climate changes, Rev. Geophys., 48, RG3001, doi:10.1029/2009RG000302, 2010. 4756

Sodemann, H. and Zubler, E.: Seasonal and inter-annual variability of the moisture sources for Alpine precipitation during 1995–2002, Int. J. Climatol., 30, 947–961, doi:10.1002/joc.1932, 2010. 4754

Sodemann, H., Masson-Delmotte, V., Schwierz, C., Vinther, B., and Wernli, H.: Inter-annual variability of Greenland winter precipitation sources. Part II: Effects of North Atlantic oscillation variability on stable isotopes in precipitation, J. Geophys. Res., 113, D12111, doi:10.1029/2007JD009416, 2008a. 4754, 4759

Sodemann, H., Schwierz, C., and Wernli, H.: Inter-annual variability of Greenland winter precipitation sources. Part I: Lagrangian moisture diagnostic and North Atlantic oscillation influence, J. Geophys. Res., 113, D03107, doi:10.1029/2007JD008503, 2008b. 4754

Steen-Larsen, H. C., Masson-Delmotte, V., Sjolte, J., Johnsen, S. J., Vinther, B. M., Breon, F.-M., Clausen, H. B., Dahl-Jensen, D., Falourd, S., Fettweis, X., Gallee, H., Jouzel, J., Kageyama, M., Lerche, H., Minster, B., Picard, G., Punge, H. J., Risi, C., Salas, D., Schwander, J., Steffen, K., Sveinbjoernsdottir, A. E., Svensson, A., and White, J.: Understanding the climatic signal in the water stable isotope records from the NEEM shallow firn/ice cores in northwest Greenland, J. Geophys. Res., 116, D06108, doi:10.1029/2010JD014311, 2011. 4757, 4768

Steffensen, J. P., Andersen, K. K., Bigler, M., Clausen, H. B., Dahl-Jensen, D., Fischer, H., Goto-Azuma, K., Hansson, M., Johnsen, S. J., Jouzel, J., Masson-Delmotte, V., Popp, T., Rasmussen, S. O., Roethlisberger, R., Ruth, U., Stauffer, B., Siggaard-Andersen, M.-L., Sveinbjornsdottir, A. E., Svensson, A., and White, J. W. C.: High-resolution Greenland Ice

CPD
9, 4745–4770, 2013

Core data show abrupt climate change happens in few years, Science, 321, 680–684, doi:10.1126/science.1157707, 2008. 4747, 4759
Stenni, B., Masson-Delmotte, V., Johnsen, S., Jouzel, J., Longinelli, A., Monnin, E., Röthlisberger, R., and Selmo, E.: An oceanic cold reversal during the last deglaciation, Science, 293, 2074–2077, 2001. 4746, 4749
Uemura, R., Matsui, Y., Yoshimura, K., Motoyama, H., and Yoshida, N.: Evidence of deuterium excess in water vapor as an indicator of ocean surface conditions, J. Geophys. Res., 113, D19114, doi:10.1029/2008JD010209, 2008. 4749, 4750, 4751, 4756, 4765, 4769
Uemura, R., Masson-Delmotte, V., Jouzel, J., Landais, A., Motoyama, H., and Stenni, B.: Ranges of moisture-source temperature estimated from Antarctic ice cores stable isotope records over glacial–interglacial cycles, Clim. Past, 8, 1109–1125, doi:10.5194/cp-8-1109-2012, 2012. 4749
Vimeux, F., Masson, V., Jouzel, J., Stievenard, M., and Petit, J. R.: Glacial-interglacial changes in ocean surface conditions in the Southern Hemisphere, Nature, 398, 410–413, 1999. 4746, 4749, 4755, 4756
Werner, M., Mikolajewicz, U., Heimann, M., and Hoffmann, G.: Borehole versus isotope temperatures on Greenland: seasonality does matter, Geophys. Res. Lett., 27, 723–726, 2000. 4756, 4759
Werner, M., Langebroek, P. M., Carlsen, T., Herold, M., and Lohmann, G.: Stable water isotopes in the ECHAM5 general circulation model: toward high-resolution isotope modeling on a global scale, J. Geophys. Res., 116, D15109, doi:10.1029/2011JD015681, 2011. 4758
Yoshimura, K., Kanamitsu, M., Noone, D., and Oki, T.: Historical isotope simulation using reanalysis atmospheric data, J. Geophys. Res., 113, D19108, doi:10.1029/2008JD010074, 2008. 4748, 4758

CPD
9, 4745–4770, 2013

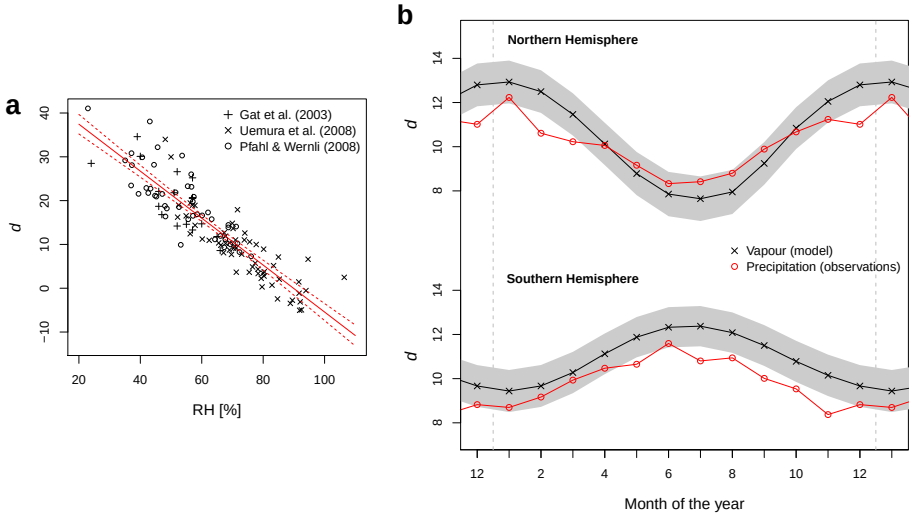

Fig. 1. Deuterium excess *d* of water vapour and precipitation. **(a)** Scatter plot of water vapour *d* from several published data sets (Gat et al., 2003; Uemura et al., 2008; Pfahl and Wernli, 2008) against RH at the oceanic moisture source. The solid red line indicates a linear regression, which is used for the calculation of moisture source *d* in our statistical model, the dashed lines show the uncertainty of this regression based on a 95 % confidence interval. **(b)** Seasonal cycle of *d* in ocean evaporation (black crosses and gray shading), as obtained from the linear regression model based on reanalysis RH, averaged over the Northern and Southern Hemisphere. Red circles show hemispherically averaged *d* of precipitation from GNIP stations.

CPD
9, 4745–4770, 2013

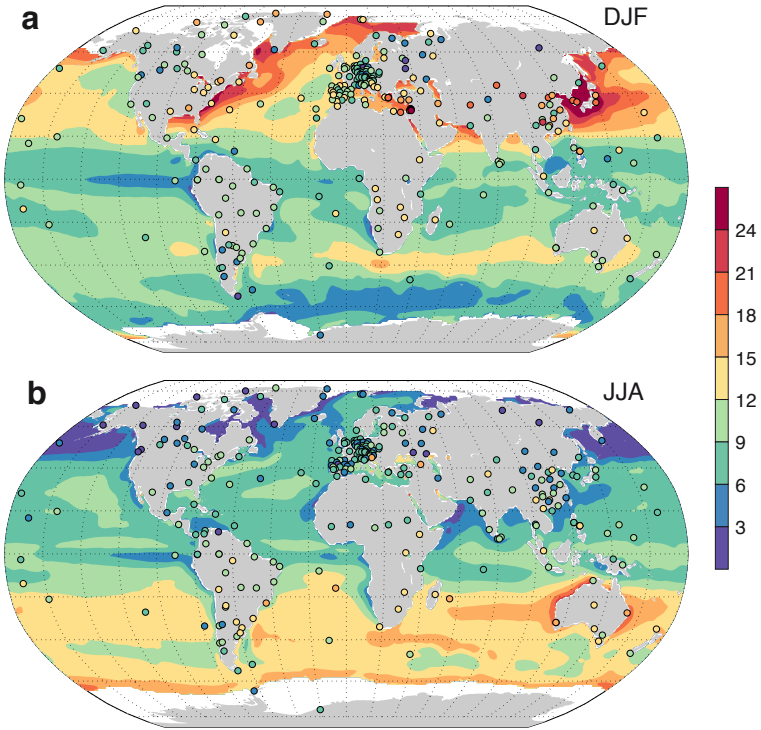

Fig. 2. Spatial distribution of predicted evaporation *d* (shading) and observed *d* in precipitation (circles). Colour shading shows seasonal mean *d* of ocean surface evaporation, as obtained from the regression model and RH from atmospheric reanalyses, for the seasons December to February **(a)** and June to August **(b)**. Regions with sea-ice in the seasonal mean are masked in white. The coloured circles show seasonal mean *d* of precipitation at GNIP stations. Note that evaporation and precipitation *d* are not expected to directly correspond, since precipitation *d* at each station is influenced by regionally varying moisture sources.

CPD
9, 4745–4770, 2013

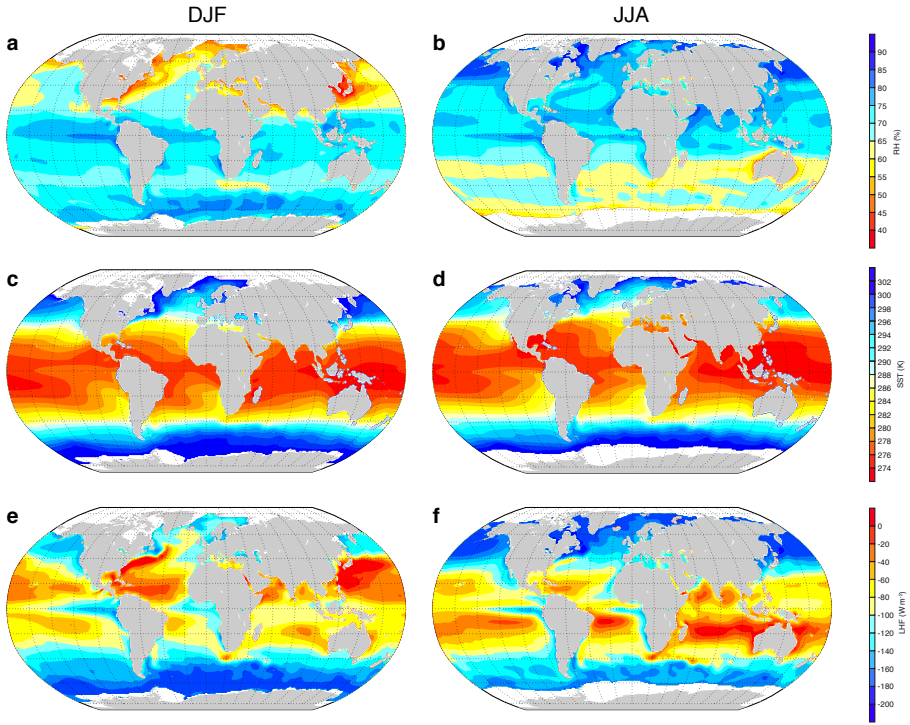

Fig. 3. Seasonal means of relative humidity over the ocean for DJF **(a)** and JJA **(b)**, sea surface temperature for DJF **(c)** and JJA **(d)**, as well as surface latent heat flux (LHF) for DJF **(e)** and JJA **(f)**. The means of both RH and SST are weighted averages, using the local LHF as a weight. Regions with sea ice in the seasonal mean are masked in white.

CPD
9, 4745–4770, 2013

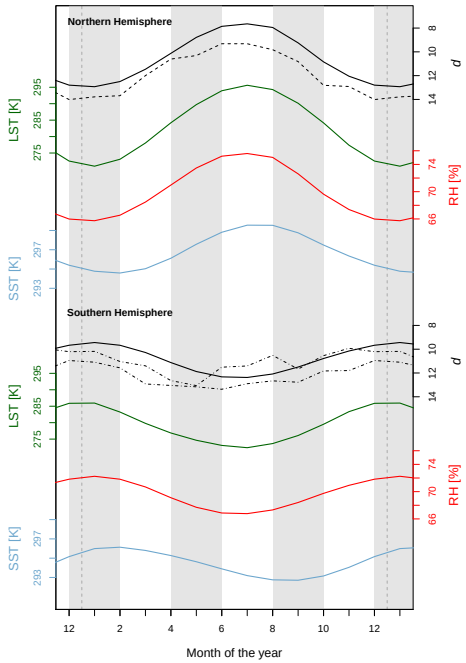

Fig. 4. Hemispheric mean seasonal cycle of predicted *d* in comparison with other variables. The black lines show the averaged *d* of ocean evaporation as predicted by the regression model. Green lines show averages of land surface temperature (LST). Mean RH over the ocean and sea surface temperature (SST), both weighted with the surface latent heat flux, are shown by red and blue lines, respectively. Seasonally resolved *d* from a shallow ice core from the NEEM site, Greenland, covering a 41 yr period (Steen-Larsen et al., 2011) is shown as dashed line. The dashed-dotted lines show the seasonal cycle from two cores from Law Dome, Antarctica, covering 12 yr (Delmotte et al., 2000) shifted by 8 ‰.

CPD
9, 4745–4770, 2013

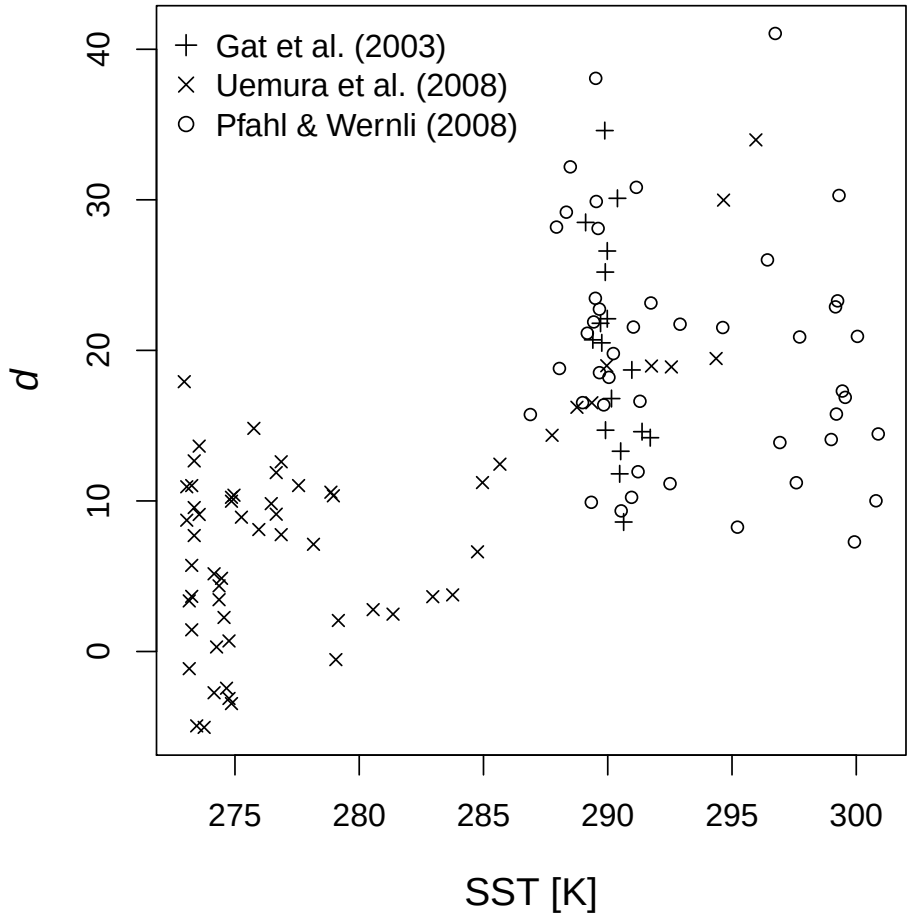

Fig. 5. Scatter plot of water vapour *d* from several published data sets (Gat et al., 2003; Uemura et al., 2008; Pfahl and Wernli, 2008) against SST at the oceanic moisture source.

CPD
9, 4745–4770, 2013

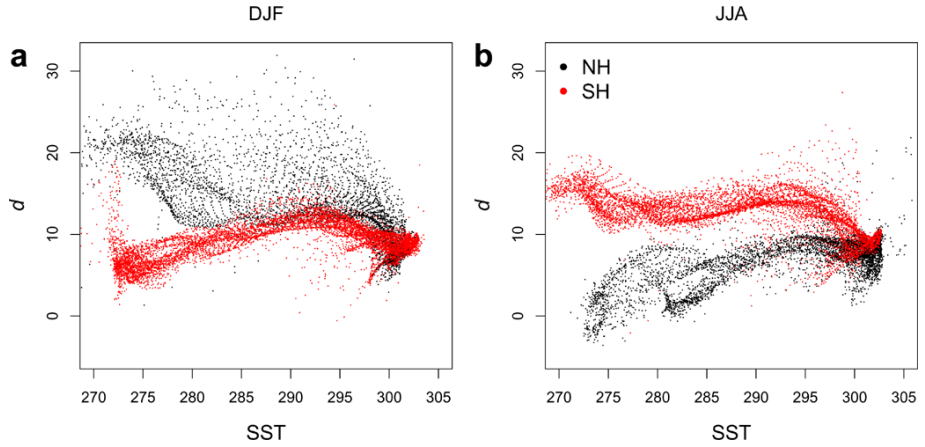

Fig. 6. Seasonal means of d as obtained from our model plotted against seasonal mean SST from the corresponding ERA-Interim grid boxes for **(a)** DJF and **(b)** JJA. For clarity, only every third point is shown.

CPD
9, 4745–4770, 2013